

Influence of Wing Shape on Airfoil Performance: a Comparative Study

HOCINE HARES¹, GHAZALI MEBARKI²

¹Department of Mechanical Engineering, LICEGS Laboratory,
University of Batna 2 Mostefa Ben Boulaid,
53, Route de Constantine. Fésdis, Batna,
ALGERIA

²Department of Mechanical Engineering, LESEI Laboratory,
University of Batna 2 Mostefa Ben Boulaid,
53, Route de Constantine. Fésdis, Batna,
ALGERIA

Abstract: - The aerodynamic performance of an aircraft mainly depends on the lift force, drag force, and the lift to drag ratio. The geometric shapes of aircraft wings are considered crucial for this aerodynamic performance. The purpose of this study is to determine the most efficient wing shape that improves the aerodynamic performance of the airfoil. For that purpose, a numerical comparative study was carried out between the rectangular and tapered wing shapes of the NACA 4412 airfoil for a wide range of angles of attack in the subsonic regime. ANSYS Fluent software, based on the finite volume method, was used for the numerical resolution of the governing equations. The Realizable k- ϵ model was chosen for the turbulence modeling. The numerical procedure was validated based on experimental results obtained from the literature. The results show an improvement in the lift coefficient and a reduction in the drag coefficient of the Tapered shape compared to the rectangular shape at all angles of attack. However, a gain was achieved in the lift-to-drag coefficient ratio of the Tapered shape.

Key-Words: - Rectangular wing, Tapered wing, Aerodynamic performance, Drag, Lift, Airfoil.

Received: October 18, 2022. Revised: August 8, 2023. Accepted: September 19, 2023. Published: October 6, 2023.

1 Introduction

The aerodynamic performance of the airfoil has an important influence during the development of airplanes. The main role of the wing shape is to generate a lift force greater than the force of gravity and to minimize the drag force. Indeed, the performance of an airfoil depends on its aerodynamic characteristics, which are influenced by the shape and size of the wings. For that purpose, several researches have been devoted to the optimization of lift and drag forces by modifying the aircraft wing's structure. The study, [1], studied the effect of a new vortex generator configuration, delta wing shape, placed in the suction surface of a rectangular profile NACA 4412. The experimental study carried out in a wind tunnel showed an improvement in the lift coefficient with a 20% increase and a one-degree delay in the incidence stall. The improvement of the aerodynamic performance of the NACA 4415 airfoil by flow control using a passive technique was investigated [2]. This was achieved by attaching gothic-shaped vortex generators to the surface of the wing. The

results of the parametric study show an increase in the lift coefficient due to vortex generators at high angles of attack. The study, [3], experimentally investigated the effect of surface roughness features on a tapered NACA 4412 wing. They showed that the best-located wing roughness features contributing to minimum drag and maximum lift are located between 75 % and 95 % of the mean leading edge chord compared to the other locations. A comparative analysis of the aerodynamic characteristics of rectangular and curved leading edge wing planforms of the NACA 2412 airfoil was carried out, [4]. A rectangular shape with straight leading and trailing edges and a curved leading edge with a straight trailing edge were tested. Lift and drag forces were determined over a wide range of angles of attack. The results show that the curved leading edge wing planform has a higher coefficient of lift and a lower coefficient of drag. Experimental investigations have been conducted on the performance of the NACA 4412 wing with a curved leading edge, [5]. A rectangular model with straight leading and trailing edges is compared to another model with curved leading and straight trailing

edges. It was found that the curved leading edge wing has a higher lift coefficient and lower drag coefficient than the rectangular leading edge wing. The study, [6], studied, numerically and experimentally, the improvement of the aerodynamic performance of the NACA 4412 airfoil through the modification of the leading edge. The results showed an improvement in aerodynamic performance with the curved leading edge. The study, [7], examined the morphing wings with upward and downward deflections of the leading edge at different frequencies. The numerical results show that the deflection of the leading edge has the most significant effect on the stall characteristics and the stall angle of attack increases due to the downward deflection of the leading edge. For upward deflection, the results are reversed. The study, [8], presents the experimental study on rough-wing and smooth-wing models using PIV and force measurements in wind tunnels. The rough model was based on the actual dimensions of the fully extended swift wing and compared with a smooth one. The experimental results showed that the aerodynamic performance of the roughened swift wing can be improved. An experimental analysis of the static aerodynamic stability of different wing planform types of the NACA 0016 airfoil was presented by, [9]. Rectangular, rectangular with tip curved, Tapered, and Tapered with tip curved wing were chosen for this analysis. All wings have been tested in the wind tunnel at various low speeds and different angles of attack. The tapered wing with a curved tip was found to be the most stable wing planform. The study, [10], studied the aerodynamic characteristics and the static stability of the wing-in-ground effect aircraft. The effect of geometric characteristics, namely twist angle, dihedral angle, sweep angle, and taper ratio, was investigated. The numerical results show that the lift coefficient increases and the maximum drag coefficient depends on the decrease in the ground clearance torsion angle, the dihedral angle, the angle of attack, and the torsion angle. To reduce fuel consumption, [11], presents a fuel-saving double-channel wing configuration. The main objective of this work is to improve the lift-to-drag ratio of the wing by taking advantage of the beneficial influence of the propeller on the wing. The numerical results show that the proposed wing configuration increases the lift-to-drag ratio by 13.29 % and reduces wing drag by 10.41 %, resulting in a fuel saving of 20.15%. The study, [12], developed a new airfoil design for an unmanned aerial vehicle by using CFD to analyze the performance of six combined wing designs. The results show that the best blended-

winglet configuration is the 0.3 taper ratio combination, as it improves the average lift-to-drag ratio by 9.84 % while reducing the average wingtip vortex by 17 %. The study, [13], studied the improvement of the aerodynamic performance of fixed-wing unmanned aerial vehicles operating in the low-speed subsonic regime. Based on the results of the aerodynamic investigations, an in-depth review of drag reduction technologies is carried out based on the existing literature, and the most promising technologies are proposed. The study, [14], used the 'wing smarting' approach to study the effects of twist angle variation on aerodynamic coefficients and the flow field. A specific range of angles of attack and twist angles was investigated. The results show that the aerodynamic efficiency is relatively related to the increase in twist angle and improves over a wide range of angles of attack.

In the present study, a numerical study is carried out to investigate the effect of wing shape on the performance of the NACA 4412 airfoil. For this purpose, two wing shape models (rectangular and conical) were tested. The aim was to compare the effectiveness of the deformation structure on the aerodynamic profiles.

2 Mathematical Formulation

In this study, the fluid was assumed to be Newtonian and incompressible. The fluid flow has been considered stationary, three-dimensional, and turbulent. The governing equations are given by:

$$\frac{\partial U_i}{\partial X_i} = 0 \quad (1)$$

$$U_j \frac{\partial U_i}{\partial X_j} = -\frac{1}{\rho} \frac{\partial P}{\partial X_i} + \frac{1}{\rho} \frac{\partial}{\partial X_j} (\mu \frac{\partial U_i}{\partial X_j} - \overline{\rho U_i U_j}) \quad (2)$$

The Reynolds stress equation is given by

$$-\overline{\rho U_i U_j} = \mu_t (\frac{\partial U_i}{\partial X_j} + \frac{\partial U_j}{\partial X_i}) - \frac{2}{3} \rho k \delta_{ij} \quad (3)$$

$$\mu_t = \rho C_\mu \frac{k^2}{\varepsilon} \quad (4)$$

For turbulence modeling, the Realizable k-ε turbulence model was chosen. It is characterized by the following equations:

$$\frac{\partial}{\partial t} (\rho k) + \frac{\partial}{\partial X_j} (\rho k U_j) = \frac{\partial}{\partial X_j} \left[(\mu + \frac{\mu_t}{\sigma_k}) \frac{\partial k}{\partial X_j} \right] + P_k + P_b - \rho \varepsilon - Y_M + S_k \quad (5)$$

$$\frac{\partial}{\partial t} (\rho \varepsilon) + \frac{\partial}{\partial X_j} (\rho \varepsilon U_j) = \frac{\partial}{\partial X_j} \left[(\mu + \frac{\mu_t}{\sigma_\varepsilon}) \frac{\partial \varepsilon}{\partial X_j} \right] + \rho C_1 S_\varepsilon - \rho C_2 \frac{\varepsilon^2}{k + \sqrt{V \varepsilon}} + C_{1\varepsilon} \frac{\varepsilon}{k} C_{3\varepsilon} P_b + S_\varepsilon \quad (6)$$

The constant values are given by:

$$C_{1\varepsilon}=1.44, C_2=1.9, \sigma_k=1, \sigma_\varepsilon=1.2$$

The Aerodynamic coefficients are given by:

$$C_p = (P - P_0) / (\rho U_\infty^2 / 2) \quad (7)$$

$$C_L = F_y / (\rho S U_\infty^2 / 2) \quad (8)$$

$$C_D = F_x / (\rho S U_\infty^2 / 2) \quad (9)$$

For the boundary conditions, at the inlet; the velocity is assumed to be equal to 34 m/s, corresponding to a 2.17×10^5 Reynolds number.

At the outlet, according to the fully developed flow regime, the following parameters are imposed:

$$\frac{\partial U}{\partial y} = 0, \quad \frac{\partial P}{\partial y} = 0, \quad \frac{\partial T}{\partial y} = 0 \quad (10)$$

At the top and bottom of the domain symmetrical conditions are imposed.

3 Profile Shape Design Overview

SolidWorks software was used to design the NACA4412 profile for both configurations (Rectangular and Tapered shapes). The chord length for the rectangular wing is 0.1 m, while for the Tapered wing, two different chords are used, 0.1 m and 0.025 m. Both shapes have a wingspan of 0.15m (Figure 1 and Figure 2).

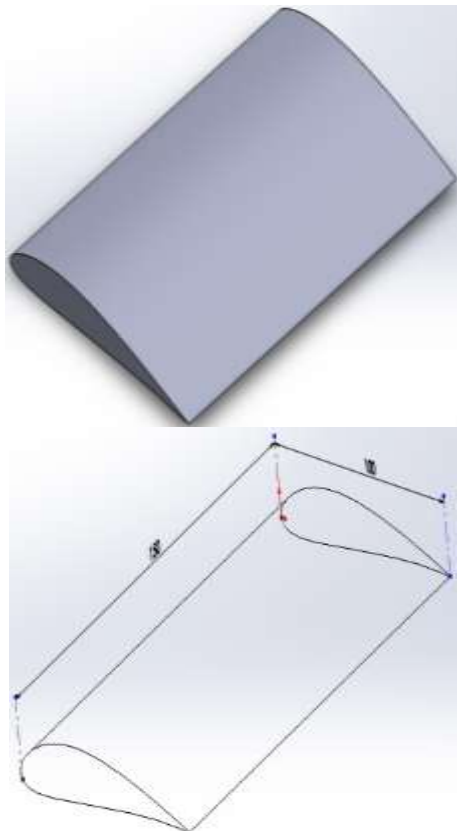


Fig. 1: Rectangular planform design

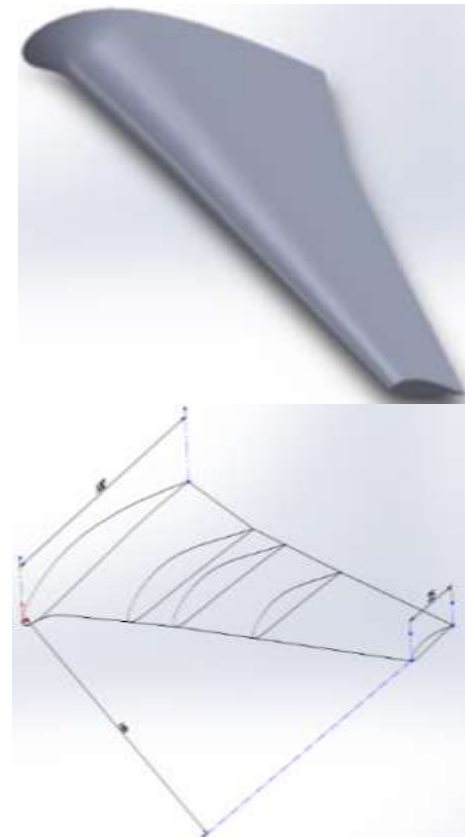


Fig. 2: Tapered planform design

4 Numerical Resolution Procedure

Fluent software, based on the finite volume method, was used to numerically solve the above mathematical equations. The SIMPLE algorithm was used to resolve the pressure-velocity coupling. In contrast, the pressure-based solver, the standard pressure interpolation scheme, and the implicit formulation method were chosen. The second-order upwind scheme was adopted in the momentum equation discretization to obtain more accurate results.

4.1 Mesh Independence Study

A mesh-independence study was performed to select an optimal number of elements to ensure that the solution obtained is mesh-independent. The independence of the mesh size has been evaluated by varying the lift, drag, and lift-to-drag ratio coefficients. For this purpose, two different types of mesh (tetrahedral and polyhedral) with different degrees of refinement have been tested. The details of the tetrahedral mesh are given in Table 1. The conversion of tetrahedral meshes to polyhedral meshes was evaluated to reduce the number of elements in the tetrahedral mesh. Polyhedral mesh details are given in Table 2.

Table 1. Tetrahedral mesh details

Types	Elements numbers	Nodes numbers
Tetrahedral 1	1466189	256514
Tetrahedral 2	2170055	378944
Tetrahedral 3	3492362	603809
Tetrahedral 4	9092704	1552911

Table 2. Conversion of tetrahedral to polyhedral meshes

Types	Elements numbers	Nodes numbers
Polyhedral 1	248969	1406517
Polyhedral 2	393796	2259657
Polyhedral 3	619195	3596170
Polyhedral 4	1569187	9240635

Figure 3, Figure 4, and Figure 5 show the lift, drag, and lift-to-drag ratio coefficient variations with the angle of attack obtained by numerical simulation compared to those obtained by, [1].

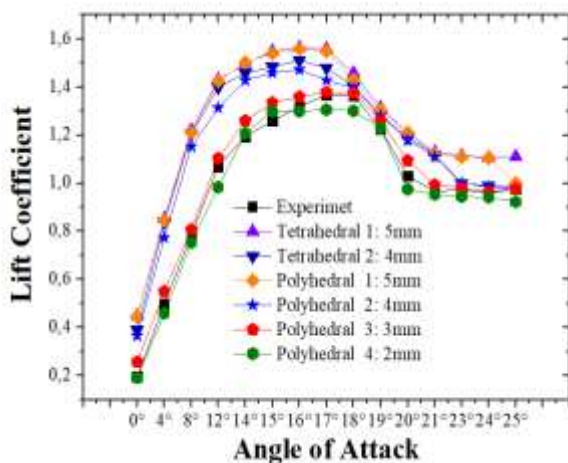


Fig. 3: Lift coefficient for different mesh sizes compared with the results of, [1]

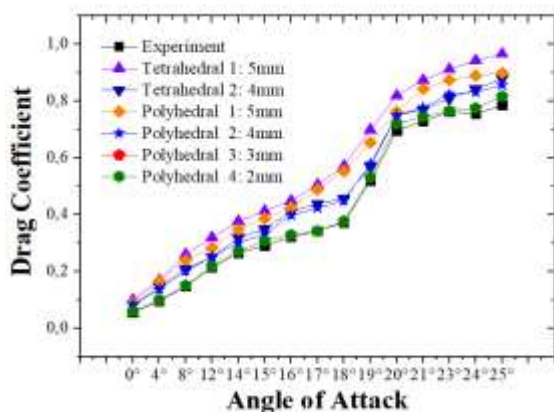


Fig. 4: Drag coefficient for different mesh sizes compared with the results of, [1]

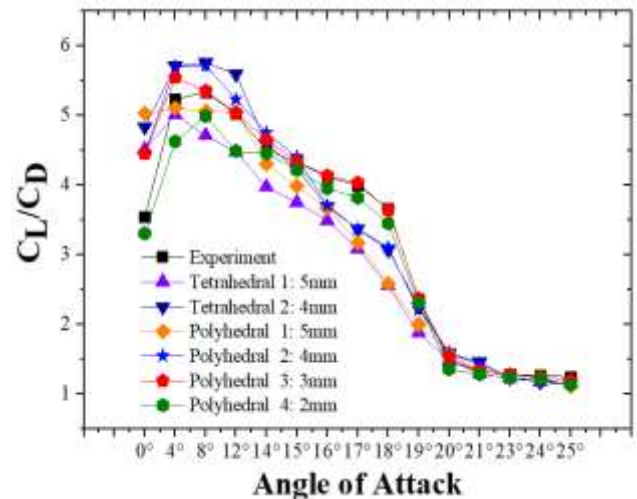


Fig. 5: Lift-to-drag coefficient for different mesh sizes compared with the results of, [1]

A good agreement is observed between the experimental results of, [1], and the refined polyhedral meshes of 2 mm and 3 mm. However, the 3 mm refined mesh is adopted because it contains fewer elements than the 2 mm refined mesh for optimum computation time. The domain used in this study is shown in Figure 6 and the chosen mesh is shown in Figure 7 and Figure 8.

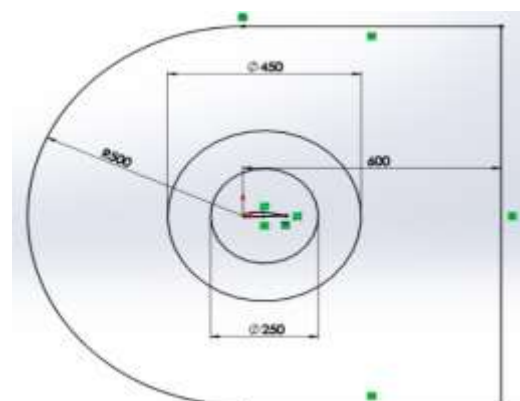


Fig. 6: Control domain dimension in (mm)

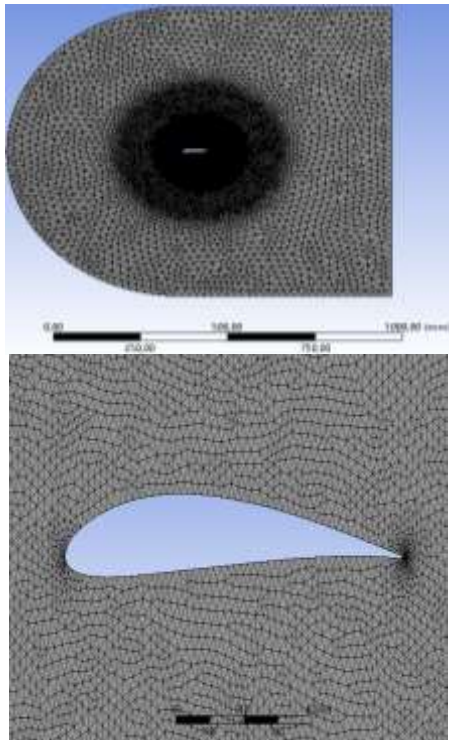


Fig. 7: The used mesh

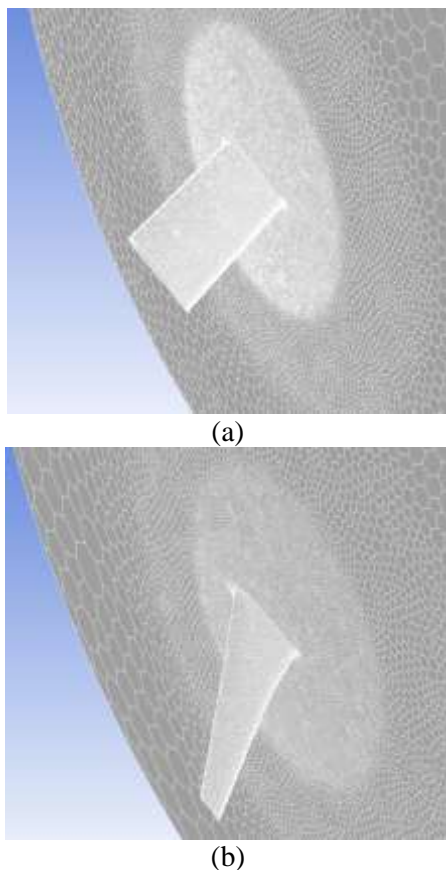


Fig. 8: Polyhedral mesh: (a) Rectangular planform, (b) Tapered planform

4.2 Turbulence Modeling

Two well-known turbulence models ($k-\epsilon$ Realizable and Spalart-Allmaras) were tested to determine the best turbulence model. The numerical results were compared with those obtained by, [1].

It is clear from Figure 9, Figure 10 and Figure 11 that a good agreement was obtained with the $k-\epsilon$ Realizable turbulence model. Consequently, our numerical procedure was validated and the Realizable $k-\epsilon$ turbulence model was adopted in the present study.

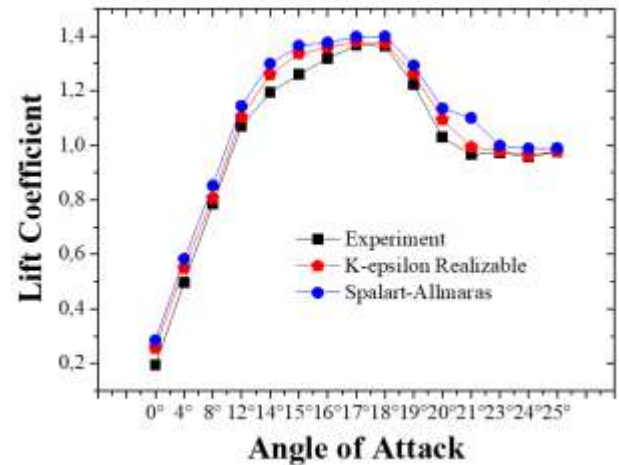


Fig. 9: Lift coefficient for different turbulence models compared to, [1] results

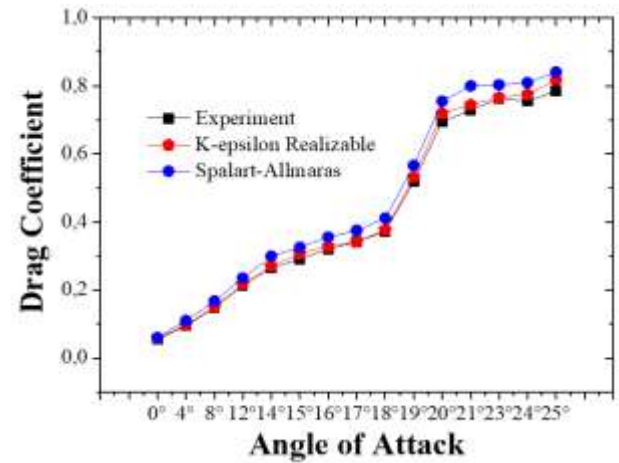


Fig. 10: Drag coefficient for different turbulence models compared to, [1] results

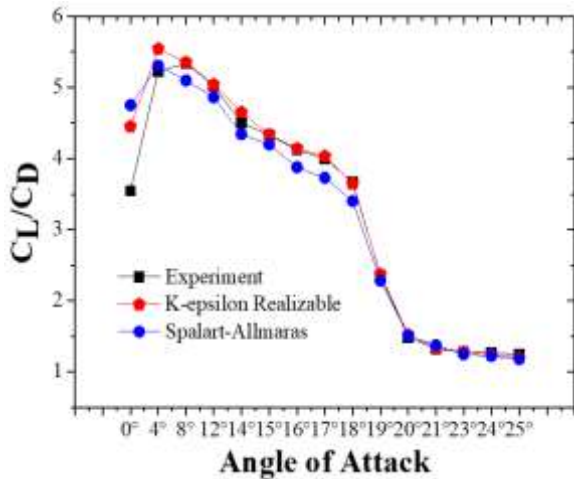


Fig. 11: Lift-to-drag coefficient for different turbulence models compared to, [1] results

5 Results and Discussion

The lift and drag coefficients as a function of angle of attack for the rectangular and tapered planform wings are shown respectively in Figure 12 and Figure 13. It is clear that both shapes have the same drag coefficient. However, the lift coefficient of the tapered wing shape is higher than that of the rectangular shape, especially at high angles of attack (from 20° to 25°). The aerodynamic performances have been improved by the tapered wing shape at all angles of attack (0° to 25°) compared to the rectangular wing shape, as shown by the lift-to-drag coefficient ratio (Figure 14).

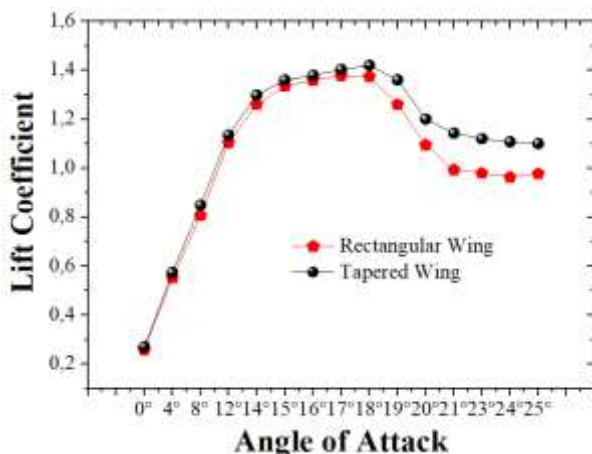


Fig. 12: Lift coefficient for rectangular and tapered wing planforms

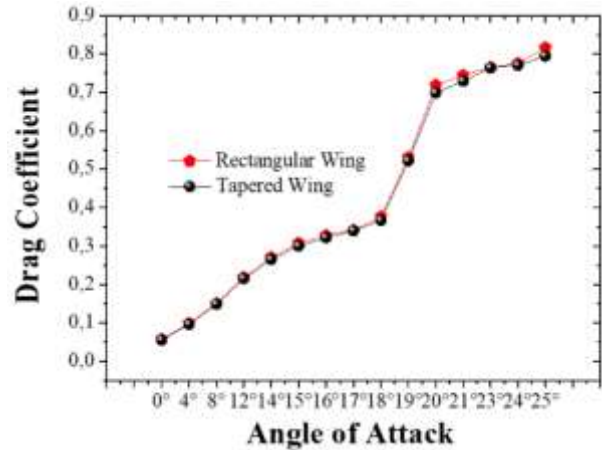


Fig. 13: Drag coefficient for rectangular and tapered wing planforms

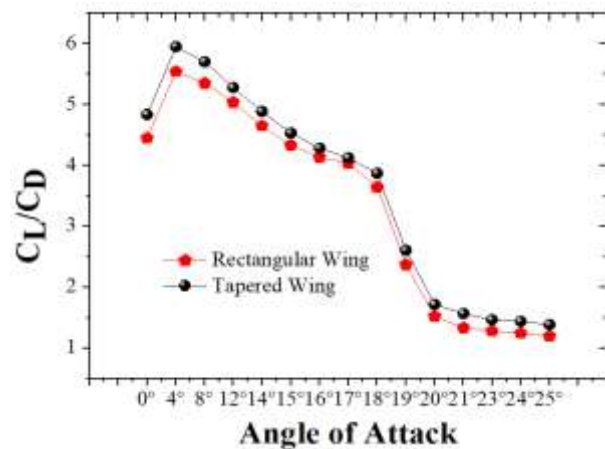


Fig. 14: Lift-to-drag coefficient ratio for rectangular and tapered wing planforms

Velocity contours around tapered and rectangular wings at different angles of attack and for two wing chord positions (20 % and 80 %) are shown in Figure 15. It can be seen that at zero angles of attack, the same velocity contours are observed for both positions, with a very small variation. As the angle of attack increases, the recirculation zone (flow separation) at the trailing edge of the wing becomes significant, especially at large positions (80%). At low positions (20%), the recirculation zone is reduced for tapered wings.

Pressure contours around tapered and rectangular wings at different angles of attack and for two wing chord positions (20 % and 80 %) are shown in Figure 16. At zero angle of attack the same tendency is observed for both wing shapes. However, the pressure distribution is strongly affected at high angles of attack. In this case, lower pressures on the upper wing surface and higher pressures on the bottom wing surface are obtained for tapered wings.

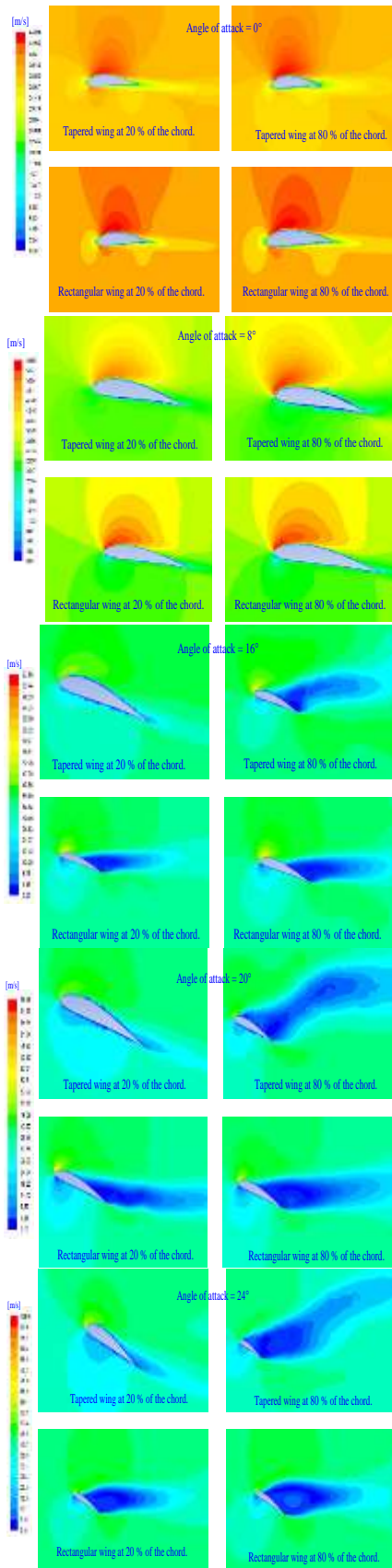


Fig. 15: Velocity contours around tapered and rectangular wings for different angles of attack and at two wing chord positions (20 % and 80 %).

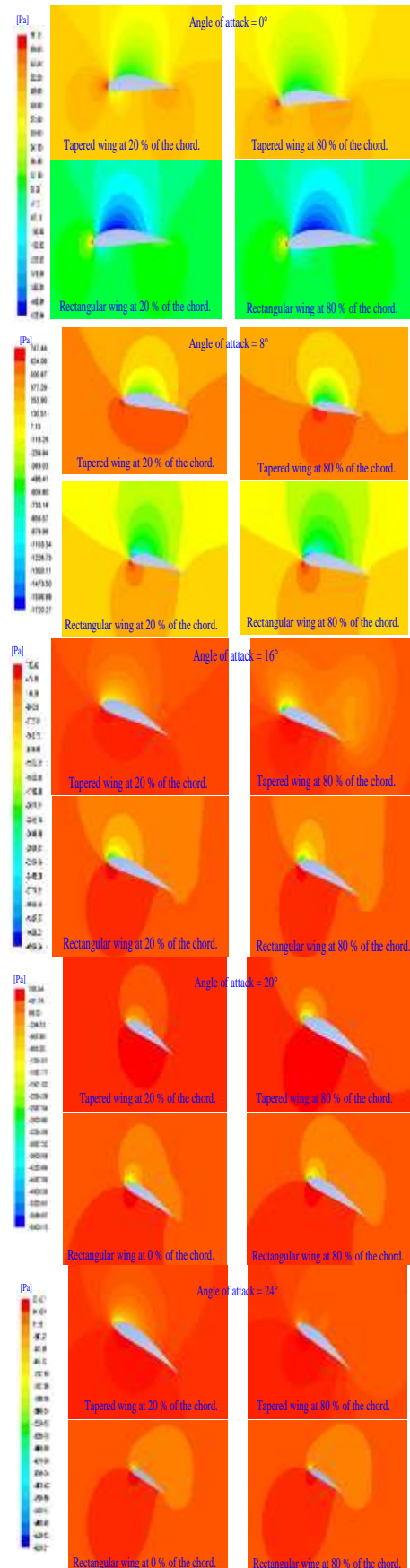


Fig. 16: Pressure contours around tapered and rectangular wings for different angles of attack and at two wing chord positions (20 % and 80 %).

6 Conclusion

In this paper, a numerical comparative study of the shape geometry was performed of the NACA 4412 airfoil for two configurations, the rectangular and the Tapered planforms. The numerical procedure using Fluent software has been validated by the experimental results. The numerical results show that the tapered wing improves the lift coefficient and reduces the drag coefficient at high angles of attack (from 20° to 25°) compared to the rectangular wing. In addition, the improvements in aerodynamic performance at all angles of attack (from 0° to 25°) are shown by the lift-to-drag ratio for the tapered wing shape. In addition, alternative aircraft design techniques such as roughened surfaces, ailerons, and multi-element wings could be explored to improve the aerodynamic performance of airfoils. It is also worth investigating these techniques to determine the most cost-effective and size-appropriate method. Alternatively, vortex generators on aircraft wings are suggested to improve their aerodynamic performance.

References:

- [1] H. Tebbiche, M. S. Boutoudj, Passive control on the naca 4412 airfoil and effects on the lift, *Conference proceeding: Design and Modeling of Mechanical Systems*, Vo.II, 2015, pp.775-78.
- [2] H. Hares, G. Mebarki, M. Brioua, and M. Naoun, Aerodynamic performances improvement of NACA 4415 profile by passive flow control using vortex generators, *Journal of the Serbian Society for Computational Mechanics*, Vol.13, No.1, 2019, pp.17-38.
- [3] K. Malik, M. Aldheeb, W. Asrar, and S. Erwin, Effects of bio-inspired surface roughness on a swept back tapered NACA 4412 wings, *Journal of Aerospace Technology and Management*, Vol.11, 2019, pp.1719 (1-15)
- [4] Md. I. K. Monirul, A. Al-Faruk, Comparative analysis of aerodynamic characteristics of rectangular and curved leading edge wing planforms, *American Journal of Engineering Research*, Vol.7, No.5, 2018, pp.281-291.
- [5] M. Nazmul Haque, M. Ali, I. Ara, Experimental investigation on the performance of naca 4412 aerofoil with curved leading-edge planform, *Procedia Engineering*, Vol.105, 2015, pp.232- 240.
- [6] B. Ravi Kumar, Enhancing aerodynamic performance of NACA 4412 aircraft wing using leading edge modification, *Wind and Structures*, Vol.29, No.4, 2019, pp.271-277.
- [7] Zi Kan., L. Daochun, S. Tong, X. Jinwu, and Z. Lu, Aerodynamic characteristics of morphing wing with flexible leading-edge, *Chinese Journal of Aeronautics*, Vol.33, No.10, 2020, pp.2610-2619.
- [8] V. B. Evelien, D. K. Roeland, E. E. Gerrit, and L. David, Feather roughness reduces flow separation during low Reynolds number glides of swifts, *Journal of Experimental Biology*, Vol.218, No.20, 2015, pp.3179-3191.
- [9] D. D. Yagya, P. M. Satya, D. Satyadhar, Experimental aerodynamic static stability analysis of different wing planforms, *Internat. Journal of Advancements in Research & Technology*, Vol.2, No.6, 2013, pp.1-4.
- [10] M. Tahani, M. Masdari, A. Bargestan, Aerodynamic performance improvement of WIG aircraft, *Aircraft Engineering and Aerospace Technology*, Vol.89, No.1, 2017, pp.120-132.
- [11] H. Wang, W. Gan, D. Li, An Investigation of the Aerodynamic Performance for a Fuel Saving Double Channel Wing Configuration, *Energies*, Vol.12, No.20, 2019, pp.3911 (1-16).
- [12] D. D. P. D. Tjahjana, I. Yaningsih, B. Y. L. Imama and A. R. Prabowo, Aerodynamic Performance Enhancement of Wing Body Micro UAV Employing Blended Winglet Configuration, *Evergreen Joint Journal of Novel Carbon Resource Sciences & Green Asia Strategy*, Vol.08, No.04, 2021, pp.799-811.
- [13] P. Panagiotou, K. Yakinthos, Aerodynamic efficiency and performance enhancement of fixed-wing UAVs, *Aerospace Science and Technology*, Vol.99, 2020, pp.105575 (1-13).
- [14] R. K. Kelayeh, M. H. Djavareshkian, Aerodynamic investigation of twist angle variation based on wing smarting for a flying Wing, *Chinese J. of Aeronautics*, Vol.34, No.2, 2021, pp.201-216.

Contribution of Individual Authors to the Creation of a Scientific Article (Ghostwriting Policy)

- Ghazali Mebarki, Methodology and initial design.
- Hocine Hares, Simulation and interpretation.

Sources of Funding for Research Presented in a Scientific Article or Scientific Article Itself

No funding was received for conducting this study.

Conflict of Interest

The authors have no conflict of interest to declare.

Creative Commons Attribution License 4.0 (Attribution 4.0 International, CC BY 4.0)

This article is published under the terms of the Creative Commons Attribution License 4.0

https://creativecommons.org/licenses/by/4.0/deed.en_US